Effects of bed slope on the flow field of vertical slot fishways

Quaranta E.[1], Katopodis C[2], Comoglio C.[3]

[1,3] *Politecnico di Torino, DIATI (Department of Environment, Land and Infrastructure Engineering).*
Corso Duca degli Abruzzi 24, 10129, Torino, Italia

[2] *Katopodis Ecohydraulics Ltd., Winnipeg, Canada*

Abstract

Vertical Slot Fishways (VSF) are the most efficient and least selective typology of technical fish passage, due to their ability to remain effective even when significant upstream and/or downstream water level fluctuations occur. Fishway construction costs can be reduced by increasing its bed slope, but this affects the flow field inside the pools, with higher head drops between the basins, as well as turbulence levels and flow velocities, which may affect fish passage. In light of this, a vertical slot fishway (VSF) was investigated by 3D numerical simulations to identify the possible effects of the bed slope (using values from 1.67% to 10%) on the flow field, and subsequent implications for fish passage. A particular focus was devoted to cyprinind species, but results can be extended to other species of similar swimming abilities and therefore, be applicable to multispecies rivers. Flow velocity and turbulence values like turbulent kinetic energy and Reynolds stresses were analyzed from a fish passage perspective in relation to threshold values derived from previous studies. Pool areas where turbulence values are compatible with fish ability and behavior were quantified. Maps of the location of fish friendly zones in the VSF pools were

*[1](corresponding author). emanuele.quaranta@polito.it, quarantaemanuele@yahoo.it Tel: 0039 0110905682

**[2]KatopodisEcohydraulics@live.ca

[3] claudio.comoglio@polito.it

produced and can constitute a reference for practical applications in fishway design. The flow field generated with bed slopes lower than 6.67% is more compatible with fish swimming capabilities, since it exhibits a predominantly 2D behavior and more suitable hydraulic conditions whereas, at higher slopes, turbulence levels in the pools increase.

Keywords: bed slope, ecohydraulics, fish passage, fishway, vertical slot fishway

1. Introduction

The interruption of longitudinal connectivity of a natural river by anthropogenic obstructions is perceived as one of the main causes in the decline of freshwater ichthyofauna (Calles and Greenberg, 2009). With the aim of restoring to an acceptable level the longitudinal connectivity of a river, the construction of fishways represents the best practice where obstacle removal is not feasible.

The flow field and turbulence level in a fishway affect the capability of fish to successfully migrate through it (Silva et al., 2011 and 2015). Shear stresses and hydrodynamic resistance generated by flowing water and turbulence on fish body make migration an energetically demanding process. Therefore, the design of a fishway has to take into account the biological characteristics of the migrating fish, i.e their swimming capability, size and fish reaction to external stimuli like turbulence, flow acceleration and velocity (Clay, 1995; Rodriguez et al., 2006; Katopodis and Gervais, 2016; Katopodis and Williams, 2012; DWA, 2014). In Clay (1995), Katopodis and Gervais (2016), Katopodis and Williams (2012), Plaut (2012), Puertas et al. (2012), Silva et al. (2011 and 2015), Tuhtan et al. (2018), Tritico and Cotel (2010), Quaranta et al. (2017) the interaction between fish and flow field in fish passes has been investigated and discussed.

Pool-and-weir fishways are the most common type of technical fish passage device

(Hatry et al., 2016; Santos et al., 2016), consisting of a channel with a sloping bed divided into a series of pools by cross-walls at regular intervals. The most efficient and least selective typology of pool-and-weir fish passage is the Vertical slot fishway -VSF-, consisting of a sloping rectangular channel divided into a number of pools by vertical baffles. Water flows through the vertical slot between the baffles, from one pool to the downstream one. Vertical slot fishways have the advantage of allowing fish to move from one pool to the next without having to jump, being able to swim at any desired depth (Cordoba et al., 2018). Under uniform flow conditions, the water level difference Δh between two adjacent pools depends on the slope of the fishway i and on the length L of the pool, i.e. $\Delta h = iL$. VSFs remain effective even when upstream and/or downstream water level fluctuations occur (Katopodis, 1992). VSFs are recommended especially in rivers where several fish species with different swimming capabilities are present (FAO, 2002; Stuart and Berghuis, 2002; DWA, 2014).

The most seminal work on VSF design was presented in Rajaratnam et al. (1992), where eighteen different designs of VSF were physically tested. Among the investigated designs, Design 1 -D1- is the most common and represents the standard reference typically used in real applications. The geometry of D1 suggested in Rajaratnam et al. (1992) has a slot orientation $\alpha = 45°$ (i.e. the angle between the width of the slot and the longitudinal direction). Taking the slot width b_0 as reference, suggested pool dimensions are $L = 10b_0$ and $B = 8b_0$, where L is the length and B is the width of the pool (Fig.1).

In addition to b_0, B and L, another important parameter in the design of a VSF is the bed slope i. The higher the slope, the lower the costs, since fewer pools are required for a certain head difference. However, for higher bed slopes, the turbulence and flow velocities can increase to levels that impair fish passage efficiency. Furthermore, the topology of the flow field is affected by the slope: bed slope values higher than 10% are commonly considered not fish friendly (Chorda et al., 2010). The bed slope and the pool length determine the head drop Δh between adjacent pools, which is a reference parameter for fishway design, being related to the maximum flow velocity through the slots. Different Δh values are recommended for different biocoenotic regions along the river, according to the swimming capabilities of the target species (DWA, 2014).

1.1. Range of VSF bed slopes for practical applications

In general, to ensure good ecological efficiency, the bed slope should guarantee a 2D flow pattern, because high vertical velocity components are likely to disturb fish performance (Wang et al., 2010). If a jet impacts the side-wall of a pool (that generally happens at slopes higher than 10% when the standard dimensions are used, (Rajaratnam et al., (1992)) a swirl is created with a horizontal axis that generates high-velocity vertical components. The formation of recirculation zones, that are too large and that drive the jet in the direction of the baffle, has to be avoided (Wang et al., 2010). Hence 5% slope is considered appropriate for multispecies rivers to limit species selectivity and to ensure a predominant 2D flow field (Marriner et al., 2016; Quaranta et al., 2017), while 10% is a value used to limit fishway construction costs, especially when passage of larger Salmonids or other species of similar swimming ability and behaviour, is expected.

However, there is no clear ecological assessment of VSF for different slopes in the literature. The general question is whether a given bed slope configuration can determine hydrodynamic conditions affecting fish pass efficiency. Field experiments on the ecological efficiency of VSF found in the literature (Laine at al., 1998; Romao et al., 2017; Thiem et al., 2013; Stuart and Cooper, 1999; Duarte et al., 2012; Silva et al., 2015) show that for bed slopes lower than 5%, fish passage efficiency is generally higher than 30% and in certain cases higher than 60% (Stuart and Cooper, 1999; Duarte et al., 2012; Thiem et al., 2013; Silva et al., 2015), while it falls below 30% at higher slopes (Laine at al., 1998; Quaresma et al., 2017; Romao et al., 2017; Romao et al., 2018). Based on experiments in non uniform flow conditions, fish were found making broader use of the fishway pool in scenarios with lower water drops, which are highly correlated with regions of overall lower turbulence and velocity magnitude (Fuentez-Perez et al., 2018). However, geometric and hydraulic configurations of these field experiments significantly differ from each other, not allowing a clear assessment of fish behavior in relation to bed slope. Furthermore, each study tested only one bed slope configuration, making it difficult to generalize results.

On the other hand, experimental and numerical studies on the hydraulic of VSFs at different slopes generally involved only a few slopes, typically 5%, 10% and 15%, with no results for intermediate slopes. In addition, areas compatible with fish rest, based on threshold values available in the literature, were not highlighted (Liu et al., 2006; Tarrade et al., 2008; Chorda et al., 2010; Wang et al., 2010).

In Chorda et al. (2010), Tarrade et al. (2008) and Wang et al. (2010), bed slopes of 5%, 10% and 15% were investigated. At 5% slope, a smaller downwelling jet and a longer jet core occurred, while the turbulence in the lower part of the pool and in the main recirculation zone was less pronounced. Furthermore, at 15% slope, low velocity areas were substantially limited, thus excluding this steep setup for practical applications. Threshold values distribution inside the pool was not discussed, and 3D turbulence effects were not considered. Considering the optimal pool dimensions ($L = 10b_0$ and $B = 8b_0$ according to Rajaratnam et al., 1992), at 5% slope the flow field comprised of a well identified jet and two large recirculating areas on its sides, while at 10% slope the left eddy split into two smaller ones, as also found in Quaranta et al. (2018), and at 15% slope the jet impacted on the left wall, completely changing the flow field by making it more complex. Liu et al. (2006) confirmed such result on design 18 -D18- presented in Rajaratnam et al. (1992), showing that at 10% slope the flow field substantially changed, and the water jet impacted against the wall creating conditions not suitable for fish.

Bed slopes lower than 5%, have been investigated by Li et al. (2017), who focused on water depths and 1D water profiles, instead of the flow field which may be more important for fish. Furthermore, the benefit gained at slopes below 5% might not justify the increase in construction costs.

Therefore, with limited hydraulic results from the literature, along with fish tests on only a few slopes and geometric configurations, it is difficult to provide a clear assessment of hydrodynamic variations in relation to the bed slope. In order to improve the knowledge on the effect of bed slope on the flow field and on its potential implications on fish passage efficiency, the present study will investigate the flow field of the standard VSF design D1 (according to Rajaratnam et al. 1992) at different bed slopes, testing six bed slopes between 1.67% and 10%. Higher slopes will not be considered due to their limited passage efficiency, as highlighted in all literature results. The distribution of turbulence parameters inside the pool will be analyzed, in order to determine the pool zones considered suitable for fish passage or rest, according to threshold values derived by previous laboratory experiments (described in section 2.1). In order to provide results directly applicable to VSFs design, the pool dimensions and the tested slopes correspond to head drop values between adjacent pools ranging from 5 to 30 cm, covering the typical range of Δh used in practical applications (e.g. DWA, 2014, Larinier, 2002).

2. Materials and Methods

Although turbulence can be numerically resolved in its different scales using direct numerical simulations (DNS), this approach is computationally too demanding. Therefore, RANS and LES methods are the most reasonable alternatives. The majority of studies have implemented RANS methods as a numerical technique for the 3D modeling of VSF, since these have shown to be capable of providing a compromise between accuracy and computational cost (Fuentes-Perez et al., 2018). Therefore, in this study a Computational Fluid Dynamic (CFD) RANS model was used. The CFD model was based on the commercial software Ansys Fluent, and it has been validated against experimental data (head-discharge and flow field) in Quaranta et al. (2017). Three momentum equations (one equation for each cartesian coordinate) and the continuity equation were solved.

The VOF (Volume of Fluid) method was used to determine the free surface position (Quaranta et al., 2017). The Reynolds shear stresses (RS) in the momentum equations $\tau_{i,j}$ were modeled by means of the turbulent dynamic viscosity μ_t:

$$\tau_{i,j} = -\rho\overline{v_i'v_j'} = \mu_t\left(\frac{\partial V_i}{\partial x_j} + \frac{\partial V_j}{\partial x_i}\right) - \frac{2}{3}\rho k \delta_{ij} \qquad (1)$$

where μ_t is the turbulent dynamic viscosity, ρ is water density, k is the turbulent kinetic energy and δ_{ij} is the Kronecker delta (Ansys Manual, 2018). The fluctuating component v_i' of velocity in direction x_i is the difference between the instantaneous value of velocity and the average velocity V_i.

The $k-\epsilon$ Realizable model was used to model the turbulent viscosity since it performs better than the standard $k-\epsilon$ model for recirculating flows (Ansys Fluent manual, 2018). The turbulent viscosity is expressed as a function of turbulent kinetic energy k and turbulent dissipation ϵ.

$$\mu_t = \rho C_\mu \frac{k^2}{\epsilon} \tag{2}$$

where $C_\mu = 0.09$.

Turbulent kinetic energy TKE is defined as $k = 1/2[{u'_i}^2 + {u'_j}^2 + {u'_w}^2]$. u'_i, u'_j, ${u'_w}^i$ are the fluctuating velocities, i.e. the differences between the instantaneous flow velocities and the mean flow velocities along the corresponding direction i, j and w. In the present case, $i = x$ (longitudinal direction), $j = y$ (transversal direction) and $w = z$ (vertical direction).

The pressure-velocity coupling was solved by PISO scheme. Spatial discretizations were realized by the following schemes: PRESTO for pressure and QUICK for momentum and turbulent kinetic energy, in alignment with Barton et al. (2008). The Curvature correction was added to sensitize the model to streamline curvatures. The numerical simulations were run in stationary and uniform conditions (same water level in the pools).

The geometric domain was made of five pools, plus a headrace and a tailrace 12 m long. The geometric dimensions of each pool were the standard ones, $L = 10b_0$ long and $B = 8b_0$ wide, where $b_0 = 0.3$ m is the slot width. The average pool water level was $y_0 = 2$ m under the uniform scenario, and six different bed slopes were investigated. The flow rate was imposed at the inlet, based on y_0 and geometry (Rajaratnam et al, 1992), while the water depths at the inlet and at the outlet were set to ensure a water depth of $y_0 = 2$ m at the center of the pool. This method was used and validated in Quaranta et al. (2017). As initial condition, all the volume was filled with air, and only at the inlet a water surface was imposed. Table 1 shows, for each slope value, the resulting head difference Δh between two adjacent pools and the flow rate Q for $y_0 = 2$ m.

A tetrahedral mesh was generated, with cell dimensions ranging between 0.025 m and 0.05 m, that is considered a good mesh to simulate hydraulic structures affecting fish behavior. Such mesh size is comparable with mesh dimensions typically used in literature (Khan, 2006; Marriner et al., 2014; Quaranta et al., 2017), and hydraulic phenomena (like eddies) are of one order of magnitude larger than mesh dimensions.

2.1. Examined variables and threshold values

Results were discussed in relation to the central pool, which is generally used as a representative reference in CFD fishways modeling (Khan, 2006; Heimerl et al., 2008; Quaranta et al., 2017). The flow field was examined on a deeper plane H_b (bottom plane) located at $0.33y_0$ (representing the flow field for bottom oriented fish species), and on a plane H_t (top plane) located at $0.67y_0$ (flow field faced by fish swimming in the upper portion of the water column). This approach was similar to Silva et al. (2012), and was useful to compare results with those found in Quaranta et al. (2017) for Design 16, which is the simplified version of the design investigated here (D1).

The examined turbulent variables were the turbulent kinetic energy TKE, the power dissipation D_ϵ and the Reynolds shear stresses RS (more specifically the tangential Reynolds stress $\tau_{x,y}$). Furthermore, the flow topology at different slopes was also analyzed along a vertical plane passing through the center of the slots, in order to better evaluate up- and downwelling phenomena.

Typical threshold velocity values recommended in fish resting zones are 0.2-0.4 m/s; this range is recommended for Cyprinids to rest before a subsequent upstream movement through higher velocity areas (Silva et al., 2012 and 2015, where fish 15-35 cm long were tested). Since Marriner et al. (2016) found that flow velocities must be kept under 0.30 m/s in 30% to 50% of the pool's volume, in this study the upper reference velocity value was taken as 0.3 m/s.

For TKE, a large portion of the pool should stay below 0.05 m^2/s^2, since higher values might affect fish passage (Marriner et al., 2016; Quaranta et al., 2017). In Romao et al. (2017), average TKE values occurring during Cyprinid passage (Iberian barbel *Luciobarbus bocagei* and Southern Iberian chub *Squalius pyrenaicus*) through a VSF ranged between 0.05 m^2/s^2 and 0.1 m^2/s^2. Therefore, preferable TKE values used in this study stay below 0.05 m^2/s^2, while 0.1 m^2/s^2 was considered a maximum acceptable limit.

With regards to RS, on the horizontal plane Iberian barbel occupied positions with absolute RS between $20 - 60$ N/m^2 (Silva et al., 2011), so that 60 N/m^2 can be considered the upper reference threshold (in Romao et al., 2017, average RS were estimated to be about 30 N/m^2 in a regular pool). Note that the upper limit 60 N/m^2 may not be enough to cause injuries or mortalities, which typically occur at much higher levels ($>$ 700 N/m^2) (Silva et al., 2011).

Finally, the power dissipation inside the pool, defined as $D_\epsilon = \frac{1}{V_p}\int_{V_p} \rho\epsilon dV_p$, where dV_p is the infinitesimal pool wet volume and ϵ is the dissipation of turbulence coming from the turbulent model, was evaluated. Usually, for the sake of simplicity in the design of technical fishways, the global volumetric dissipated power D_V is used as a reference parameter, calculated as $D_V = \frac{P}{V_p}$ where $P = \rho g Q \delta h$ (ρ is water density, g is gravity, Q is the flow rate and δh is the head difference). In general, $D_V > D_\epsilon$, since D_V includes all power losses and friction losses, not only the turbulent ones computed with D_ϵ. However, D_ϵ allows the determination of the dissipation distribution inside the pool, while D_V is just a global pool parameter (Chorda et al., 2010). Analyzing D_ϵ, the pool area was subdivided according to the the following threshold values: 1) D_ϵ= 200 W/m^3: highly turbulent areas not suitable for fish resting, where generally fish use burst speed to pass through slots (Liu, 2004); 2) 150-200 W/m^3: acceptable for larger salmonids; 3) 100-150 W/m^3 acceptable for most cyprinids species; 4) $\leq$ 100 W/m^3 conservative upper threshold for fish species with weaker swimming ability (ICPDR, 2013; Larinier, 2002).

Flow velocity and turbulent values were discussed by considering absolute local values (like maximum values), and averaged values ($\overline{V}$, $\overline{RS}$ and $\overline{TKE}$). Velocity and turbulence results were quantitatively described distinguishing between jet and low-velocity areas. Finally, based on threshold values reported within the current section 2.1, pool areas considered fish friendly were quantified and their topology within the VSF pool is presented.

3. Results and discussion

Figures 2-3 show the flow field in the pool by means of flow velocity vectors on the planes H_b and H_t. Along the plane H_b, a well visible jet and low-velocity areas on its sides are present. It can be noticed that the left eddy is progressively shifted downstream; at i=6.67%, it disappears reappearing again at i=10% splitted into two smaller ones, in agreement with Tarrade et al. (2008). As reported in Romao et al., (2018), turbulent flow fields with vortices of various sizes represents an additional difficulty for fish passage, especially for small individuals with limited swimming ability; therefore, VSFs with 10% slope are not recommended. The absence of the vortex at i=6.67% and 8.33% is due to the increased vertical component of velocities, i.e. upwelling and downwelling phenomena. This implies a higher level of turbulence in the vertical plane. Instead, the right eddy tends to be quite stable as the bed slope changes, except at i=10% where it approaches a more circular shape. Looking at the plane H_t in Fig.3, the left eddy is initially circular and located upstream. At i=5% it becomes elliptical and moves downstream, splitting into two smaller ones at i=6.67-8.33%. In all cases, average jet flow velocities are generally smaller than the maximum theoretical ones V_m, while locally maximum effective values could be slightly higher than V_m. Furthermore, as also shown in Wang et al. (2010), there is an increase in flow velocity near the left wall of the pool and in the proximity of the main transversal baffle, due to the rotation of the big vortex on the left of the pool.

When looking at a longitudinal vertical plane passing through the center of the slot (Fig.4), it can be seen that flow velocities increase from the center of the pool towards the slot downstream; this is because, in the downstream portion of the pool, the vertical plane intersects the main jet. Instead, in the upstream portion of the pool, the resting zone on the right side of the jet is shown, where the horizontal axis eddy generates flow velocities directed upstream as confirmed by Tarrade et al. (2008). This may help the upstream movements of fish that swim near the free surface. This hydraulic configuration does not occur at $i = 1.67\%$ and $i = 5\%$, where instead upstream pointed flow velocities appear in the lower portion of the pool. Indeed, the eddy on the right is more elongated, and the vertical plane intersects it in its internal part (flow velocities pointed downstream), while at the other slopes it is intersected in its external part, where flow velocities are directed upstream. Another interesting output is related to the zone where flow velocities start pointing downstream. At $i = 1.67\%$ and $i = 5\%$ the velocity increase starts from the upper portion of the pool, while at the other slopes from the bottom portion, and this is coherent with the rotation of the horizontal axis eddy. Therefore, at each slope and corresponding head difference, vertical flow velocities occur, i.e. up- and downwelling phenomena. The higher the slope, the higher the intensity of the vertical velocities, ranging from 0.05 V_m to 0.25 V_m, where V_m is the maximum flow velocity in the slot.

The water jet is responsible for the flow rate transport, and it has to be sensed readily by fish which will use their burst speed to move upstream along or through the jet length. Mean jet velocity and maximum flow velocities increase with the slope (Tab. 2). On the bottom plane, velocity values are generally higher, because the jet is more straight between the slots and less affected by the free surface. As the bed slope increases, maximum flow velocities pass from $\simeq$ 1 m/s to 2.6 m/s; this is an expected behavior, since as the slope increases also the flow rate increases, and thus the flow velocity. Instead, average jet values range between 0.71 m/s to 1.76 m/s from $i = 1.67\%$ to $i = 10\%$, which is a smaller range than that found for the maximum velocities, where the variation range of the mean velocity can be calculated as $\frac{\overline{V_{10\%}}-\overline{V_{1.67\%}}}{\overline{V_{1.67\%}}}$.

Same analogies can be found for TKE and RS, whose variation ranges are wider when considering maximum values (Tab. 2). TKE and RS at 10% slope are around 7 times compared to those at 1.67% slope when considering mean values, and approximately 10 times when considering maximum values. Furthermore, maximum and average values of turbulence and velocity change substantially from H_b to H_t (from bottom to top) as the bed slope increases, due to the highly 3D character of flow behavior and due to the flow rate increase.

In contrast, flow behavior in the low-velocity areas (Tab. 3) is more quiet, and average values change from H_b to H_t only at the highest slope, corresponding to i=10%. Maximum velocities in the low-velocity areas occur in the boundaries with the jet emanating from the slot. Variation ranges for the average values of TKE and RS are again around 7, and less than 10 times when considering maximum values, because in the low velocity areas flow behavior is less turbulent, and, therefore, the slope may have a lesser influence on turbulence in the low velocity areas with respect to the jet.

Results related to the extension of low velocity areas in the pool are reported in Tab. 4, showing the area percentage where effective values of flow velocity, TKE and RS are lower than threshold values (see section 2.1). In Tab. 4 the average values of velocity, TKE and RS inside the pool are also reported with reference to planes H_b and H_t.

Area percentages below threshold values decrease with bed slope increase, due to the increase in turbulence. In particular, a substantial decrease of low velocity areas occurs passing from $i = 1.67\%$ to $i = 3.33\%$ (see Tab.4). No substantial difference between the two planes (H_b and H_t) can be noticed. Fish friendly areas, i.e. areas with values below the threshold ones, are more developed when considering RS instead of TKE, showing that the threshold value of TKE= 0.05 m^2 s^{-2} is more conservative than RS=60 N m^{-2}. Nevertheless, fish friendly TKE areas are generally extended by about 30% of the pool, according to recommendations suggested in Marriner et al. (2016).

Areas with high TKE values are confined in the jet at low bed slopes (Fig.5), while at higher slopes, these start appearing downstream, because the water flow impacts on the downstream wall, and then spreads upstream. This is in agreement with Wang et al. (2010) and Liu et al. (2006). Instead, RS values higher than 60 Nm^{-2} are restricted only inside the main jet. Therefore, it is expected that fish resting would occur in the upstream part of the pool, where turbulence is lower, as confirmed in Laine et al. (1998), where it was found that fish gathered behind the baffles attempting to swim through the slot.

With regard to the power dissipation, in Tab.4 D_V is compared with D_ϵ, as suggested in Chorda et al. (2010). The maximum difference in percentage is 30% at $i = 5\%$, comparable with the values found in Chorda et al. (2010). The local power dissipation $\rho\epsilon$ along the plane is illustrated in Fig.7. The highest dissipation values occur near the slot and along the jet. Such distribution is in agreement with the RS distribution, because, in turbulent regimes, RS are those factors that generate power dissipation. The distribution of D_ϵ is also in agreement with results described in Chorda et al. (2010).

Looking at Figs.5-6, it can be seen that areas where flow velocity and turbulence values are lower than the maximum threshold ones are restricted to the water jet for bed slopes smaller than 5% (included). This means that low velocity areas are well developed, and they are suitable for fish to rest up to the 5% slope. The bed slope of 6.67% may still be considered fish friendly, although TKE values are not below threshold values.

Several hydraulic parameters used in this study were derived from research on a few Cyprinid species, especially Iberial barbel and chub (Silva et al., 2011; Romao et al., 2017). It is worthwhile to note that several groups of species display similarity in swimming performance (Katopodis and Gervais, 2016). For example, Sanz-Ronda et al. (2016), reported that two Cyprinids (barbel and nase) ascended the vertical slot easily. Moreover, the meta-analysis on swimming performance by Katopodis and Gervais (2016) grouped cyprinids and salmonids, indicating that fish of similar body length from these large groups of species have similar fish speeds. Furthermore, results from a recent field study on a vertical slot fishway, demonstrated that the Iberian barbel and another Cyprinid, the northern straight-mouth nase (*Pseudochondrostoma duriense*), performed similarly to a Salmonind, the brown trout (*Salmo trutta*), which were of similar size (Sanz-Ronda et al., 2016). These findings allow recommendations on VSF bed slope from this study to apply to a greater number of species.

4. Conclusions

The general question addressed by this study was whether a given slope configuration may allow more fish to pass; this is a complex matter, involving hydraulics and fish behavior, since the bed slope can significantly affect flow characteristics.

The limited field experiments in the recent scientific literature make it difficult to relate ecological performances of VSFs with the slope. Meanwhile, there is a lack of a clear and comprehensive flow field assessment of VSFs at different slopes since existing studies have only tested a maximum of three slopes.

Therefore, in this study the effects of bed slope on the flow field of a standard VSF type were analyzed by 3D numerical simulations, testing six bed slope values from 1.67% to 10%, corresponding to head drop values between pools commonly used in fishway design (from 5 to 30 cm). Comparison with results from existing literature indicate good agreement, validate simulated parameters and offer greater generalizations. The flow field was discussed analyzing flow velocities and turbulent variables as TKE, RS and power dissipation.

The velocity field was characterized by a main water jet with recirculating areas on the sides of the pools. These areas changed with the bed slope, both in size and flow behavior: indeed, at 6.67% and 8.33% the vortex on the left split into two smaller ones, and due to their dimensions more comparable with fish size, they could be perceived as obstacles for fish passage (Silva et al., 2012).

Low velocity areas in the pools, that are important for fish rest and energy recovery, decreased with the bed slope increase. Areas where flow velocity and turbulent values are higher than the maximum threshold ones are restricted to the water jet for bed slopes smaller that 5% (included). With the exception of TKE, the 6.67% (ΔH = 20 cm) bed slope may be considered fish friendly. Higher slopes are not recommended, because turbulence may form a barrier for migrating fish.

Therefore, the slope of 6.67% (ΔH = 20 cm) can be considered the upper limit in the design of fishways except for larger salmonids or species of similar swimming abilities and behavior. The 6.67% slope may be reasonable only when there is a need to reduce construction costs related to a 5% slope. Milder slopes would result in an increase in fish passage construction costs, whilst no significant improvement in the ecological efficiency would occur, and may be recommended only when passage has to be provided to species with very weak swimming abilities.It is also essential to guarantee a maximum flow velocity lower than the burst speed of fish.

5. Bibliography

Ansys Fluent. 2018. user manual.

Barton, A., Keller, R., and Katopodis, C. 2008. A free surface model of a vertical slot fishway to numerically predict velocity and turbulence distributions. *American Fisheries Society Symposium*, **61**, 1-16.

Bravo-Cordoba, FJ., Sanz-Ronda, FJ., Ruiz-Legazpi, J., Valbuena-Castro, J., and Makrakis, S. 2018. Vertical slot versus submerged notch with bottom orifice: Looking for the best technical fishway type for mediterranean barbels. *Knowledge and Management of Aquatic Ecosystems*, **122**, 120-125.

Calles, E.O. and Greenberg, L.A. 2009. Connectivity is a two-way street – the need for a holistic approach to fish passage problems in regulated rivers. *River Research and Applications*, **25**, 1268-1286.

Chorda, J., Maubourguet, MM., Rouxab, H., Larinier, M., Tarrade, L., and David, L. 2010. Two-dimensional free surface flow numerical model for vertical slot fishways. *Journal of Hydraulic Research*, **48 (2)**, 141-151.

de Freitas Duarte, B.A., Resende Ramos, I.C., and de Andrade, H. 2012. Reynolds shear-stress and velocity: Positive biological response of neotropical fishes to hydraulic parameters in a vertical slot fishway. *Neotropical Ichthyology*, **10(4)**, 813-819.

DWA-German Association for Water, Wastewater and Waste. 2014. Fischaufstiegsanlagen und fisch-passierbare bauwerke – gestaltung, bemessung, qualitätssicherung - stand: korrigierte fassung februar 2016 (isbn: 978-3-942964-91-3)).

Food and Agriculture Organization of the United Nations (FAO)
Deutscher Verband für Wasserwirtschaft und Kulturbau (DVWK). 2002. Fish passes – design, dimensions and monitoring. *Rome, FAO*.

Fuentes-Perez, J.F., Eckert, M., Tuhtan, J.A., Ferreira, M.T., Kruusmaa, M., and Branco, P. 2018. Spatial preferences of iberian barbel in a vertical slot fishway under variable hydrodynamic scenarios. *Ecological Engineering*, **125**, 131-142.

Fuentes-Perez, J.F., Silva, A.T., Tuhtan, J.A., Garcia-Vega, A., Carbonell-Baeza, R., Musall, M., and Kruusmaa, M. 2017. 3D modelling of non-uniform and turbulent flow in vertical slot fishways. *Environmental Modelling & Software*, **99**, 156-169.

Hatry, C., Binder, TR., Thiem, JD., Hasler, CT., Smokorowski, KE., Clarke, KD., Katopodis, C., and Cooke, SJ. 2016. The status of fishways in Canada: trends identified using the national canfishpass database. *Rev. Fish Biol. Fish.*, **23**, 271-281.

Heimerl, S., Hagmeyer, M., and Echteler, C. 2008. Numerical flow simulation of pool-type fishways: new ways with well-known tools. *Hydrobiologia*, **609**, 189-196.

ICPDR. 2013. Measures for ensuring fish migration at transversal structures.

Katopodis, C. 1992. Introduction to fishway design.

Katopodis, C. and Gervais, R. 2016. Fish swimming performance database and analyses. *Fisheries and Oceans Canada*, research document - 2016/002.

Katopodis, C. and Williams, J. 2012. The development of fish passage research in a historical context. *Ecological Engineering*, **48**, 8-18.

Khan, L. 2006. A three-dimensional computational fluid dynamics (CFD) model analysis of free surface hydrodynamics and fish passage energetics in a vertical-slot fishway. *North American Journal of Fisheries Management*, **26**, 255-267.

Laine, A., Kamula, R., and Hooli, J. 1998. Fish and lamprey passage in a combined denil and vertical-slot fishway. *Fisheries Management and Ecology*, **5**, 31-44.

Larinier, M. 2002. Pool fishways, pre-barrages and natural bypass channels. *Bull. Fr. Pèche Piscic*, **364**, 54-82.

Li, G., Sun, S., Liu, H., Zheng, T., and Zhang, C. 2017. Water profiles in vertical slot fishways without central baffle. *Journal of Heat and Technology*, **35(1)**, 191-195.

Liu, M. 2004. Turbulence structure in hydraulic jumps and vertical slot fishways. *Ph.D. thesis. University of Alberta, Edmonton, CA.*

Liu, M., Rajaratnam, N., and Zhu, D. 2006. Mean flow and turbulence structure in vertical slot fishways. *Hydraulic Engineering*, **132(8)**, 765-777.

Marriner, B.A., Baki, A.B.M., Zhu, D.Z., Cooke, S.J., and Katopodis, C. 2016. The hydraulics of a vertical slot fishway: A case study on the multi-species Vianney-Legendre fishway in Quebec, Canada. *Ecological Engineering*, **90**, 190-202.

Plaut, I. 2012. Critical swimming speed: its ecological relevance. *Comparative Biochemistry and Physiology, part A*, **131**, 41-50.

Puertas, J., Cea, L., Bermúdez, M., Pena, L., Rodríguez, A., Rabunal, J.R., Balairón, L., Lara, A., and Aramburu, E. 2012. Computer application for the analysis and design of vertical slot fishways in accordance with the requirements of the target species. *Ecological Engineering*, **48**, 51-60.

Quaranta, E., Katopodis, C., Revelli, R., and Comoglio, C. 2017. Turbulent flow field comparison and related suitability for fish passage of a standard and a simplified low gradient vertical slot fishway. *River Research and Applications*, **33(8)**, 1295-1305.

Quaranta, E., Katopodis, C., Revelli, R., and Comoglio, C. 2018. Investigation of the hydrodynamic effects of bed slope in vertical slot fishways by 3d numerical simulations. *IAHR 2018, Trento, Italy, 12-14 June*.

Quaresma, A., Romao, F., Branco, P., Ferreira, M., and Pinheiro, A. 2015. Can vertical slot fishways (VSF) operate with less water without compromising effectiveness. *International Conference on Engineering and Ecohydrology for Fish Passage*, **14**.

Rajaratnam, N., Katopodis, C., and Solanki, S. 1992. New designs for vertical-slot fishways. *Canadian Journal of Civil Engineering*, **19**, 402-414.

Rodriguez, T., Agudo, J., Mosquera, L., and Gonzalez, E. 2006. Contribution of experimental fluid mechanics to the design of vertical slot fish passes. *Knowledge and Management of Aquatic Ecosystems*, **396**, 02.

Romao, F., Quaresma, A., Branco, P., Santos, J., Amaral, S., Ferreira, M., Katopodis, C., and Pinheiro, A. 2017. Passage performance of two cyprinids with different ecological traits in a fishway with distinct vertical slot configurations. *Ecological Engineering*, **105**, 180-188.

Santos, JM., Silva, AT., Katopodis, C., Pinheiro, PJ., Pinheiro, AN., Bochechas, J., and Ferreira, MT. 2016. Ecohydraulics of pool-type fishways: getting past the barriers. *Ecological Engineering*, **48**, 38-50.

Sanz-Ronda, F., Bravo-Cordoba, F., Fuentez-Perez, J., and Castro-Santos, T. 2015. Ascent ability of brown trout, salmo trutta, and two iberiancyprinids - iberian barbel, luciobarbus bocagei, and northern straight-mouth nase, pseudochondrostoma duriense- in a vertical slot fishway. *Knowledge and Management of Aquatic Ecosystems*, **417, 10**.

Silva, A., Hatry, C., Thiem, J., Gutowsky, L., Hatin, D., Zhu, D., Dawson, J., Katopodis, C., and Cooke, S. 2015. Behaviour and locomotor activity of a migratory catostomid during fishway passage. *PLoS ONE*, **10(4)**: e0123051.

Silva, A., Katopodis, C., Santos, J.M., Ferreira, M.T., and Pinheiro, A.N. 2012. Cyprinid swimming behaviour in response to turbulent flow. *Ecological Engineering*, **44**, 314-328.

Silva, A., Santos, J., Ferreira, M., Pinheiro, A., and Katopodis, C. 2011. Effects of water velocity and turbulence on the behaviour of Iberian barbel (luciobarbus bocagei, Steindachner 1864) in an experimental pool-type fishway. *River Research and Applications*, **27**, 360-373.

Stuart, I. G. and Berghuis, A. P. 2002. Upstream passage of fish through a vertical-slot fishway in an Australian subtropical river. *Fisheries Management and Ecology*, **9**, 111-122.

Stuart, I.G. and Mallen-Cooper, M. 1999. An assessment of the effectiveness of a vertical-slot fishway for non-salmonid fish at a tidal barrier on a large tropical, subtropical river. *Regul. Rivers: Res. Mgmt*, **15**, 575–590.

Tarrade, L., Texier, A., David, L., and Larinier, M. 2008. Topologies and measurements of turbulent flow in vertical slot fishways. *Hydrobiologia*, **609 (1)**, 177-188.

Thiem, J., Binder, T., Dumont, P., Hatins, D., Hatry, C., Katopodis, C., Stamplecoskie, M., and Cooke, S. 2013. Multispecies fish passage behaviour in a vertical slot fishway on the Richelieu river, Quebec, Canada . *River Research and Applications*, **29**, 582-592.

Tritico, H.M and Cotel, A.J. 2010. The effects of turbulent eddies on the stability and critical swimming speed of creek chub (semotilus atromaculatus). *Journal of Experimental Biology*, 2284-2293.

Tuhtan, J., Fuentes-Perez, J., Toming, G., Schneider, M., Schwarzenberger, R., Schletterer, M., and Kruusmaa, M. 1992. Man-made flows from a fish's perspective: autonomous classification of turbulent fishway flows with field data collected using an artificial lateral line. *Bioinspiration and Biomimetics*, **13(4)**, 046006.

Wang, R., David, L., and Larinier, M. 2010. Evaluating vertical-slot fishway designs in terms of fish swimming capabilities. *Ecological Engineering*, **27**, 37-48.

Table 1. Summary of investigated conditions: VSF bed slope i, head difference between two pools Δh and flow rate Q.

i %	$\Delta h(m)$	Q (m^3/s)
1.67	0.05	0.479
3.33	0.10	0.677
5	0.15	0.829
6.67	0.20	0.958
8.33	0.25	1.071
10	0.30	1.173

Table 2. Average and maximum values of velocity, TKE and Reynolds stresses of the jet along the planes H_b and H_t.

i %	Δh	Plane	$\overline{V}$ m/s	V_{max} m/s	$\overline{TKE}$ m^2/s^2	TKE_{max} m^2/s^2	$\overline{RS}$ N/m^2	RS_{max} N/m^2
1.67	5	H_b	0.730	0.920	0.050	0.080	11.210	41.370
		H_t	0.710	0.930	0.048	0.075	9.980	41.030
3.33	10	H_b	0.944	1.328	0.110	0.162	23.380	100.560
		H_t	0.936	1.301	0.091	0.162	18.809	104.786
5	15	H_b	1.143	1.649	0.138	0.263	38.617	259.040
		H_t	1.227	1.671	0.145	0.332	38.456	272.850
6.67	20	H_b	1.115	2.015	0.229	0.361	54.440	202.210
		H_t	1.295	1.905	0.224	0.355	47.876	209.251
8.33	25	H_b	1.342	2.248	0.285	0.438	65.970	258.680
		H_t	1.361	2.164	0.270	0.431	57.112	261.130
10	30	H_b	1.762	2.586	0.276	0.594	69.370	410.360
		H_t	1.548	2.403	0.333	0.684	79.338	469.850

Table 3. Average values of velocity, TKE and Reynolds stresses in the low velocity zones along the planes H_b and H_t.

i %	Δh	Plane	$\overline{V}$ m/s	$\overline{TKE}$ m^2/s^2	TKE_{max} m^2/s^2	$\overline{RS}$ N/m^2	RS_{max} N/m^2
1.67	5	H_b	0.180	0.023	0.081	3.980	36.72
		H_t	0.180	0.021	0.063	3.760	29.08
3.33	10	H_b	0.286	0.048	0.143	7.540	52.54
		H_t	0.275	0.045	0.146	8.241	73.03
5	15	H_b	0.321	0.055	0.184	10.176	83.67
		H_t	0.295	0.059	0.269	12.076	150.09
6.67	20	H_b	0.370	0.083	0.360	14.095	142.21
		H_t	0.393	0.092	0.285	14.865	120.08
8.33	25	H_b	0.409	0.114	0.438	20.716	162.84
		H_t	0.395	0.114	0.362	18.197	135.14
10	30	H_b	0.447	0.097	0.515	15.727	197.57
		H_t	0.333	0.147	0.570	22.535	185.62

Table 4. Area fractions inside the whole pool where values of velocity, TKE and Reynolds stresses are lower than threshold values (A_V, A_{TKE} and A_{RS}). Area fractions range from 0 to 1 (1=100%). The average flow velocity, TKE and RS on the plane are also shown, considering the whole plane (low velocity areas and jet) and values of power dissipations D_V and D_ϵ are also included (as comparison with D_V). Threshold values are 0.3 m/s, 0.05 m^2/s^2 and 60 N/m^2, respectively (Silva et al., 2011; Marriner et al, 2016).

i %	Δh	Plane	A_V -	A_{TKE} -	A_{RS} -	$\overline{V}$ m/s	$\overline{TKE}$ m^2/s^2	$\overline{RS}$ N/m^2	D_V W/m^3	D_ϵ W/m^3
1.67	5	H_b	0.750	1.000	1.000	0.233	0.025	4.67	16	16
		H_t	0.710	0.921	1.000	0.241	0.024	4.50		
3.33	10	H_b	0.496	0.470	0.992	0.373	0.056	9.63	46	35
		H_t	0.505	0.489	0.989	0.396	0.053	10.18		
5	15	H_b	0.458	0.428	0.967	0.470	0.070	15.35	85	60
		H_t	0.473	0.459	0.959	0.472	0.075	17.07		
6.67	20	H_b	0.237	0.367	0.871	0.525	0.113	22.53	131	101
		H_t	0.297	0.316	0.922	0.550	0.115	20.60		
8.33	25	H_b	0.232	0.295	0.821	0.571	0.144	28.60	182	138
		H_t	0.277	0.259	0.880	0.592	0.145	26.12		
10	30	H_b	0.289	0.282	0.870	0.760	0.140	28.51	240	194
		H_t	0.285	0.203	0.775	0.663	0.198	37.97		

List of Figures

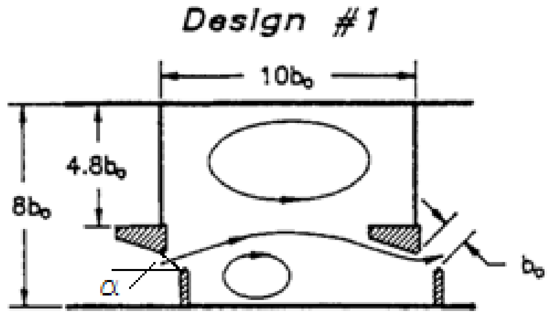

Fig. 1. Sketch of Design 1 presented in Rajaratnam et al. (1992), which is the traditional design of VSFs. In the present study, $b_0 = 0.30$ m.

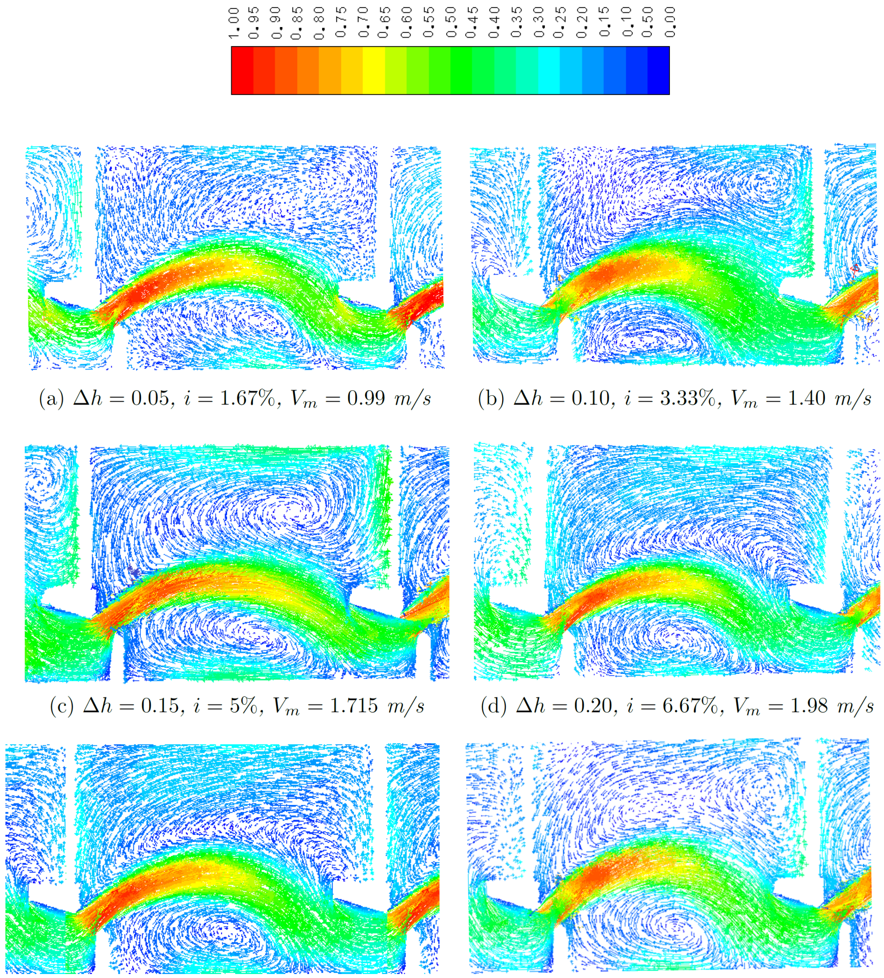

(a) $\Delta h = 0.05$, $i = 1.67\%$, $V_m = 0.99$ m/s

(b) $\Delta h = 0.10$, $i = 3.33\%$, $V_m = 1.40$ m/s

(c) $\Delta h = 0.15$, $i = 5\%$, $V_m = 1.715$ m/s

(d) $\Delta h = 0.20$, $i = 6.67\%$, $V_m = 1.98$ m/s

(e) $\Delta h = 0.25$, $i = 8.33\%$, $V_m = 2.21$ m/s

(f) $\Delta h = 0.30$, $i = 10\%$, $V_m = 2.43$ m/s

Fig. 2. Flow velocity values (normalized to the maximum flow velocity V_m for each slope) along the lower plane H_b for different bed slopes. The maximum flow velocity V_m is depicted in red and its value is reported in each figure caption, while zero flow velocity areas are in blue. Flow direction is from the left to the right.

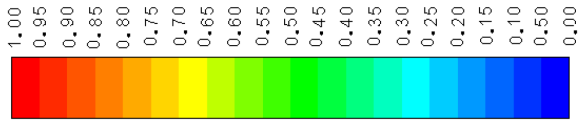

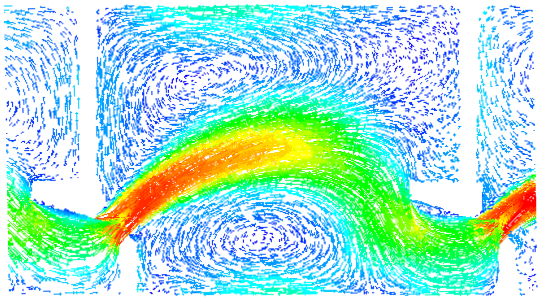

(a) $\Delta h = 0.05$, $i = 1.67\%$, $V_m = 0.99\ m/s$

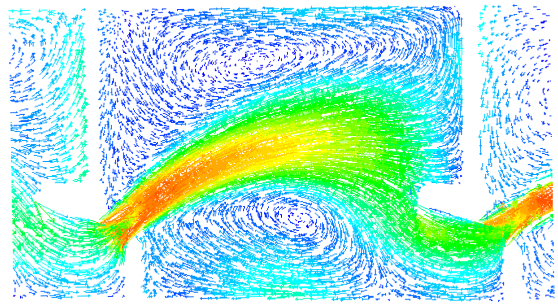

(b) $\Delta h = 0.10$, $i = 3.33\%$, $V_m = 1.40\ m/s$

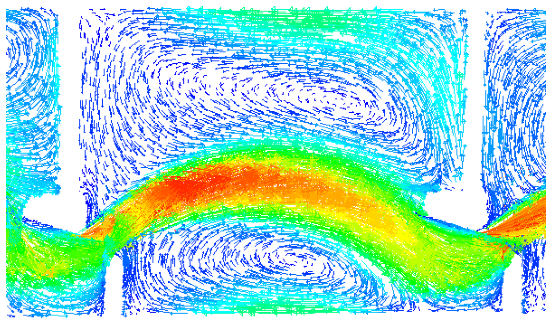

(c) $\Delta h = 0.15$, $i = 5\%$, $V_m = 1.715\ m/s$

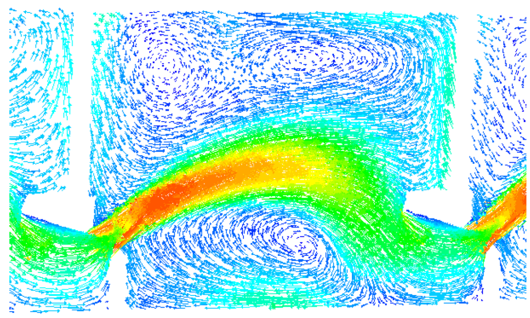

(d) $\Delta h = 0.20$, $i = 6.67\%$, $V_m = 1.98\ m/s$

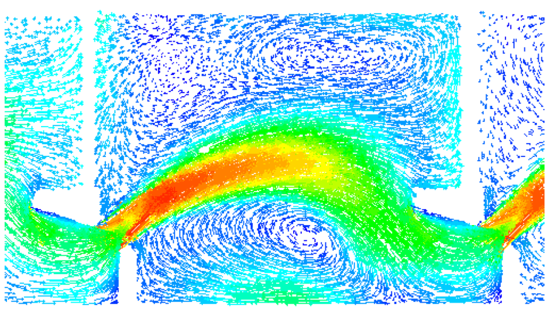

(e) $\Delta h = 0.25$, $i = 8.33\%$, $V_m = 2.21\ m/s$

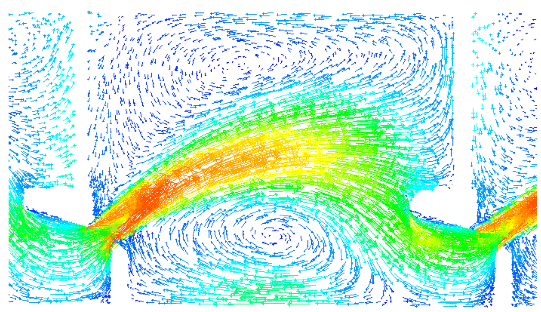

(f) $\Delta h = 0.30$, $i = 10\%$, $V_m = 2.43\ m/s$

Fig. 3. Flow velocity values (normalized to the maximum flow velocity V_m for each slope) along the higher plane H_t for different bed slopes. The maximum flow velocity V_m is depicted in red and its value is reported in each figure caption, while zero flow velocity areas are in blue. Flow direction is from the left to the right.

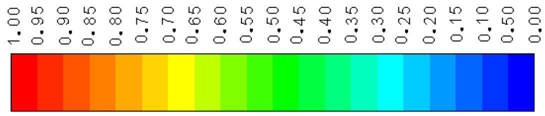

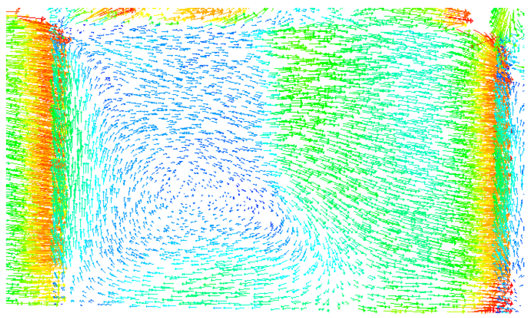

(a) $\Delta h = 0.05$, $i = 1.67\%$, $V_m = 0.99\ m/s$

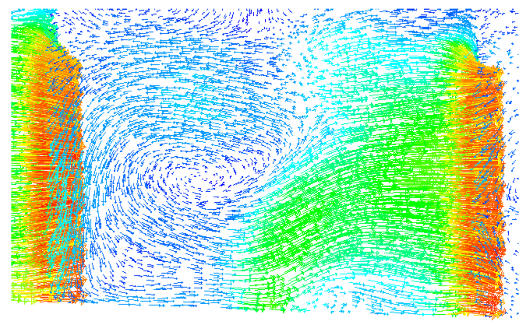

(b) $\Delta h = 0.10$, $i = 3.33\%$, $V_m = 1.40\ m/s$

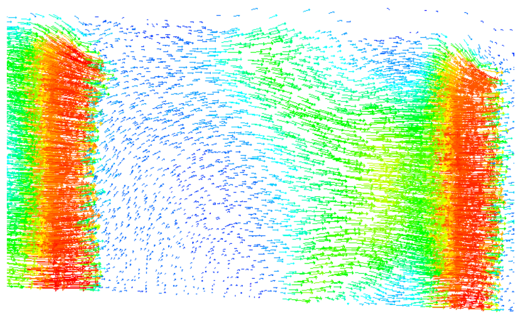

(c) $\Delta h = 0.15$, $i = 5\%$, $V_m = 1.715\ m/s$

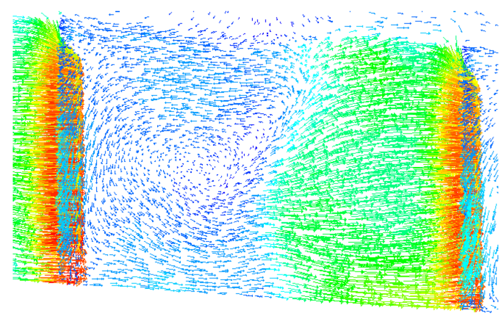

(d) $\Delta h = 0.20$, $i = 6.67\%$, $V_m = 1.98\ m/s$

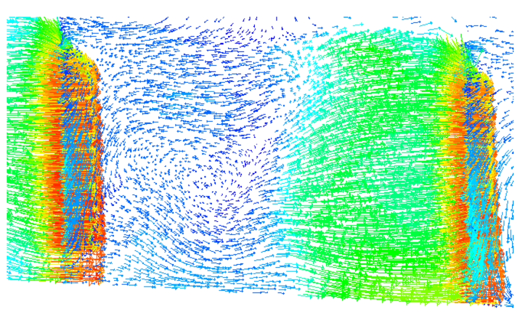

(e) $\Delta h = 0.25$, $i = 8.33\%$, $V_m = 2.21\ m/s$

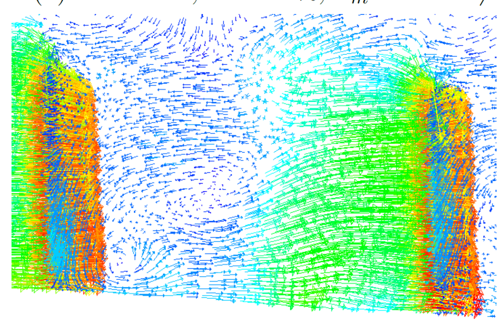

(f) $\Delta h = 0.30$, $i = 10\%$, $V_m = 2.43\ m/s$

Fig. 4. Flow velocity values (normalized to the maximum flow velocity V_m for each slope) along the vertical plane, passing for the center of the slot, for different bed slopes. The maximum flow velocity V_m is depicted in red and its value is reported in each figure caption, while zero flow velocity areas are in blue. Flow direction is from the left to the right.

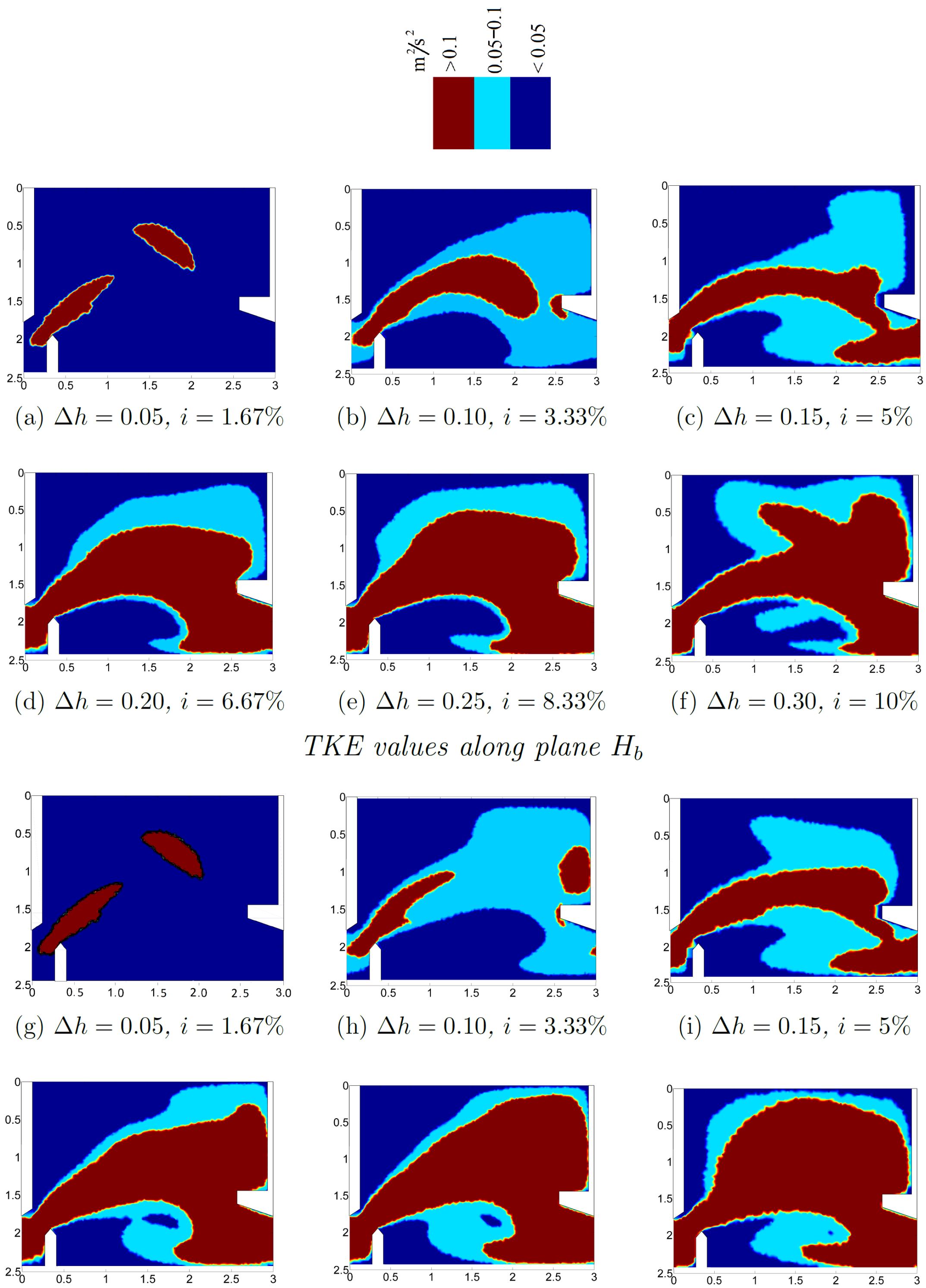

(a) $\Delta h = 0.05,\ i = 1.67\%$ (b) $\Delta h = 0.10,\ i = 3.33\%$ (c) $\Delta h = 0.15,\ i = 5\%$

(d) $\Delta h = 0.20,\ i = 6.67\%$ (e) $\Delta h = 0.25,\ i = 8.33\%$ (f) $\Delta h = 0.30,\ i = 10\%$

TKE values along plane H_b

(g) $\Delta h = 0.05,\ i = 1.67\%$ (h) $\Delta h = 0.10,\ i = 3.33\%$ (i) $\Delta h = 0.15,\ i = 5\%$

(j) $\Delta h = 0.20,\ i = 6.67\%$ (k) $\Delta h = 0.25,\ i = 8.33\%$ (l) $\Delta h = 0.30,\ i = 10\%$

TKE values along plane H_t

Fig. 5. Localization of pool zones with different TKE value ranges, along planes H_b and H_t. Flow direction from left to right.

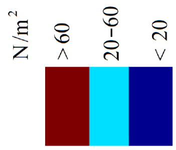

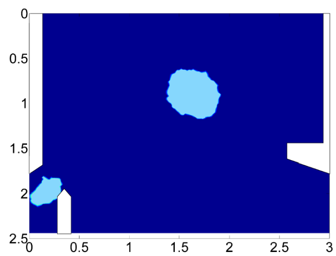

(a) $\Delta h = 0.05,\ i = 1.67\%$

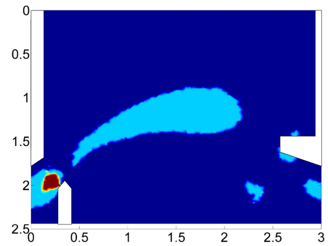

(b) $\Delta h = 0.10,\ i = 3.33\%$

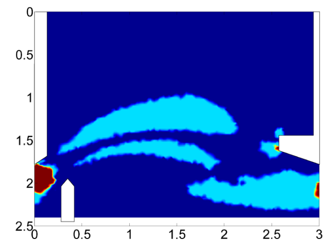

(c) $\Delta h = 0.15,\ i = 5\%$

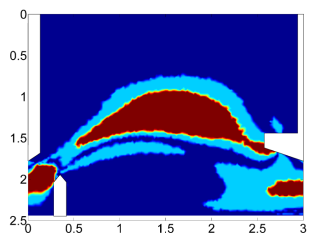

(d) $\Delta h = 0.20,\ i = 6.67\%$

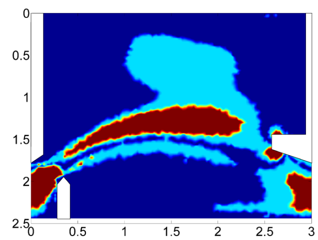

(e) $\Delta h = 0.25,\ i = 8.33\%$

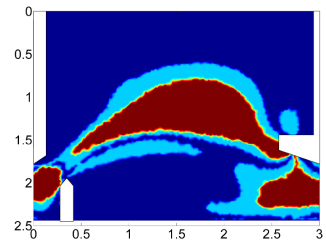

(f) $\Delta h = 0.30,\ i = 10\%$

RS values along plane H_b

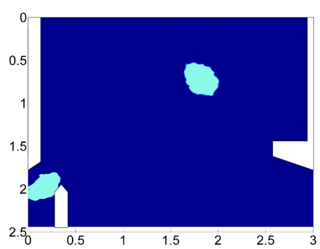

(g) $\Delta h = 0.05,\ i = 1.67\%$

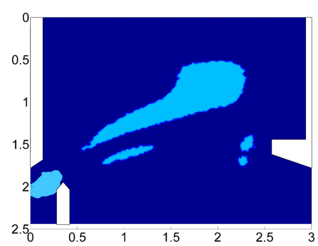

(h) $\Delta h = 0.10,\ i = 3.33\%$

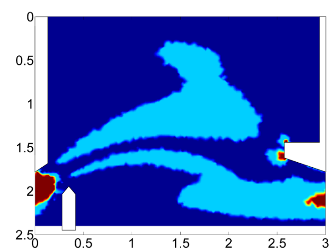

(i) $\Delta h = 0.15,\ i = 5\%$

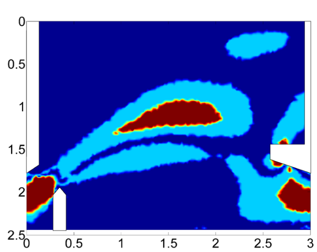

(j) $\Delta h = 0.20,\ i = 6.67\%$

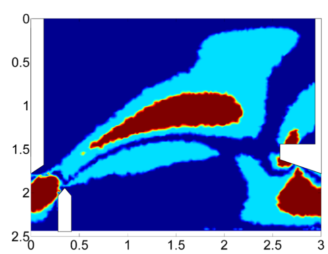

(k) $\Delta h = 0.25,\ i = 8.33\%$

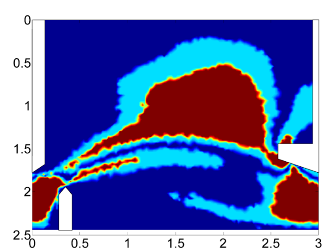

(l) $\Delta h = 0.30,\ i = 10\%$

RS values along plane H_t

Fig. 6. Localization of pool zones with different RS value ranges, along planes H_b and H_t. Flow direction from left to right.

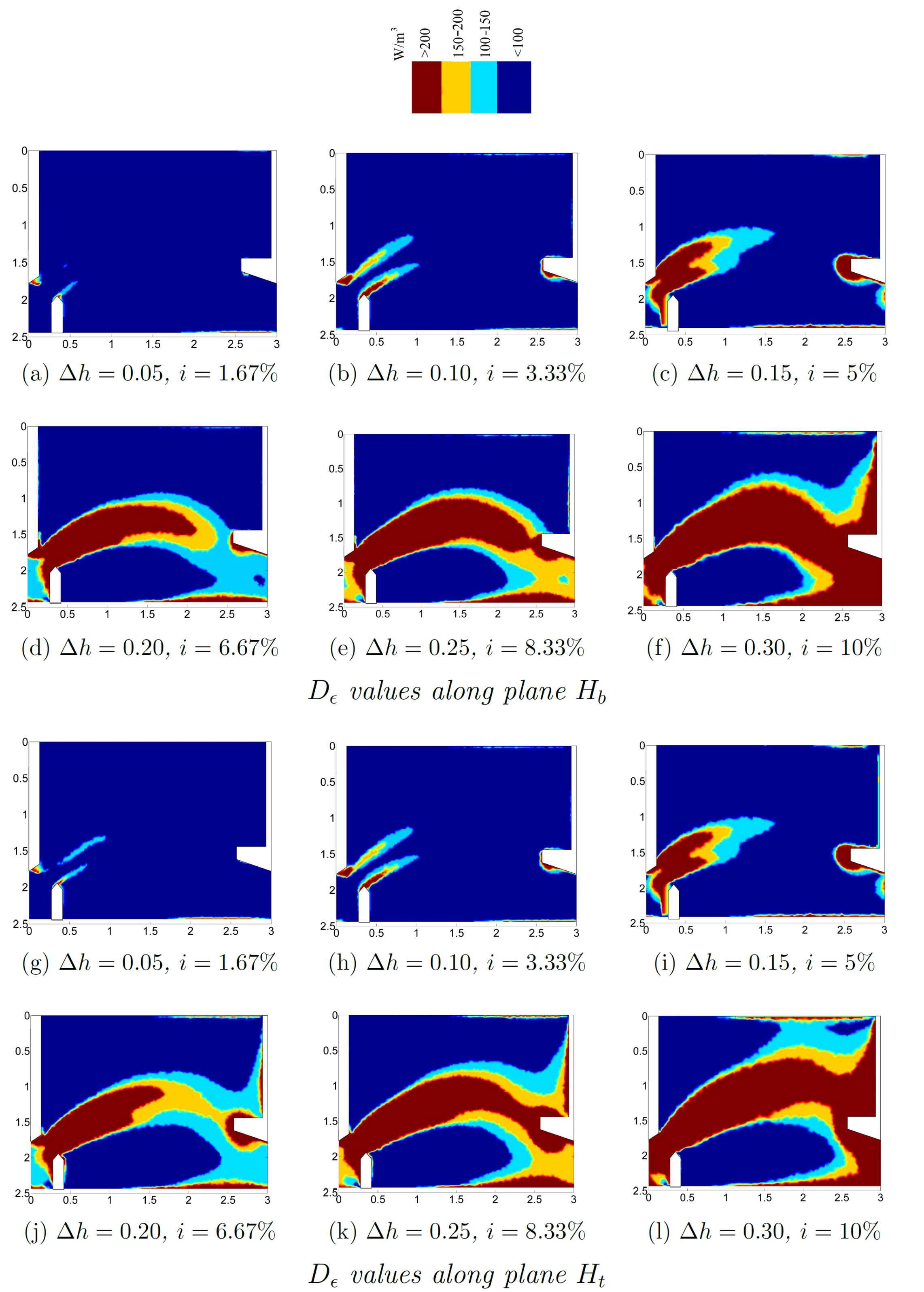

Fig. 7. Localization of pool zones with different power dissipation D_ϵ value ranges, along planes H_b and H_t. Flow direction from left to right.